Mode-Content Analysis and Field Reconstruction of Propagating Waves in Corrugated Waveguides of an ECH System

Takashi SHIMOZUMA, Hiroshi IDEI[1)], Michael A. SHAPIRO[2)], Richard J. TEMKIN[2)], Shin KUBO, Hiroe IGAMI, Yasuo YOSHIMURA, Hiromi TAKAHASHI, Satoshi ITO, Sakuji KOBAYASHI, Yoshinori MIZUNO, Yasuyuki TAKITA and Takashi MUTOH

National Institute for Fusion Science, 322-6 Oroshi-cho, Toki 509-5292, Japan
[1)]*Research Institute for Applied Mechanics Kyushu University, Kasuga, Fukuoka 816-8580, Japan*
[2)]*Plasma Science and Fusion Center Massachusetts Institute of Technology, Cambridge, MA02139, USA*

A new method is proposed to analyze the mode content of high power electromagnetic waves that are propagating through corrugated waveguides in the electron cyclotron resonance heating (ECH) systems for nuclear fusion devices. The method was applied to the 168 GHz transmission line of the ECH system in the Large Helical Device (LHD) to evaluate the waveguide alignment. The mode content of the propagating waves could be accurately analyzed using this method. Furthermore, the wave field in the waveguide was reconstructed using the mode content information obtained for each mode.

1. Introduction

Electron Cyclotron resonance Heating (ECH) is one of the most powerful heating methods for plasma heating and current drive in fusion-oriented plasma devices. High power millimeter-waves for ECH are usually transmitted through over-sized circular corrugated waveguides. The length of such a transmission line becomes longer and longer due to the huge size of plasma confinement devices. In the over-sized corrugated waveguides, a tilt and an offset of the waveguide axis easily cause the conversion of the transmitted HE_{11} mode to unwanted modes. Improving the transmission efficiency is essential in view of not only the increase in usable power, but also the reduction of the heat load to the millimeter-wave components by Ohmic loss. For example, to suppress the mode conversion loss to < 1%, the tilt angle and offset of the beam center should be less than 0.1 deg. and 2.9 mm, respectively, for the 168 GHz transmission through a corrugated waveguide with a diameter of 88.9 mm [1]. We have already proposed an alignment method of transmission lines based on infrared (IR) images on a target irradiated by high power millimeter waves [2].

As a next step, it is important to identify the mode content of the propagating waves in the corrugated waveguides for clarifying what type of misalignment induces such a mode conversion. One method of mode-content analysis which uses irradiant waveguide modes has been already proposed [3]. We will report another method of mode-content analysis and a reconstruction method of the wave field propagating in a corrugated waveguide. Figure 1 illustrates a flow chart of the mode-content analysis. At first, a target plate, which is set at a position several tens of centimeters apart from the open edge of the corrugated waveguide, is irradiated by high power millimeter waves. The temperature rise of the target plate is recorded with high precision by an IR camera at several target positions. Next, the phase information is retrieved by the phase retrieval method [4]. In parallel with this, the first and second moments of the radiation pattern are calculated to evaluate the position of the power center and the waist size of the beam. Once the information of the amplitude and phase at the exit of the waveguide is determined, the mode content can be analyzed by an orthogonal-mode expansion in the corrugated waveguide. Finally, the electric field in the waveguide can be reconstructed up to its entrance using the obtained expansion coefficients and the phase factor of each constituent mode.

This paper is organized as follows. In Sec. 2, the method of mode-content analysis is described, and the results of its application to a 168 GHz transmission line in the LHD ECH system are given. In Sec. 3, the method and calculated results of the electric field reconstruction in the corrugated waveguide are described using the information of the analyzed mode content in Sec. 2. Finally, Section 4 will be devoted to conclusions.

2. Method and Results of Mode-Content Analysis

In the process of designing phase correcting mirrors and performing waveguide alignment, the phase retrieval
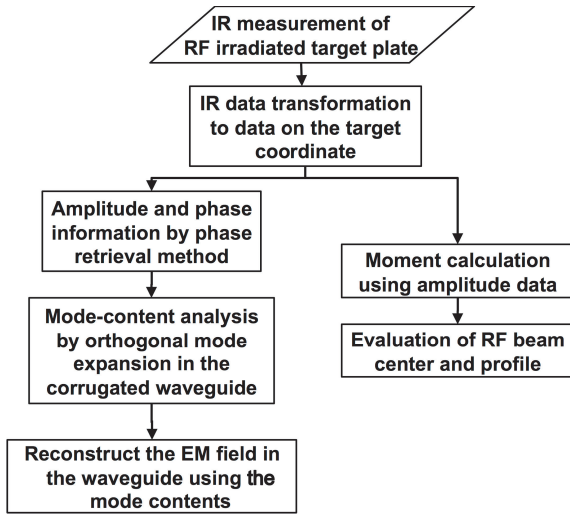
Fig. 1 A flow chart of the mode-content analysis and electric field reconstruction in the corrugated waveguide.

method was successfully used to reconstruct the phase information of the radiated waves using only measured intensity profiles at several positions [4]. By using the phase retrieval method, we can find the complex amplitude at the radiating edge of a corrugated waveguide. It can be decomposed into the eigenmodes of the corrugated waveguide. The expansion coefficients of the eigenmode give the mode content of the corresponding eigenmodes.

At the waveguide exit ($z = 0$), the phase can be retrieved by the phase retrieval method. Such amplitude $A(x, y, 0)$ and phase $\varphi(x, y, 0)$ can be expanded by the orthogonal functions in the waveguide as,

$$A(x, y, 0)e^{j\varphi(x,y,0)} = \sum_{n=1}^{N} C_n e^{j\varphi_n} \phi_n(x, y), \qquad (1)$$

where C_n is the amplitude and φ_n is the phase of a mode n. On the contrary, the expansion coefficients are represented by

$$C_n e^{j\varphi_n} = \frac{\int_S A(x, y, 0)e^{j\varphi(x,y,0)} \cdot \phi_n^*(x, y)ds}{\int_S |\phi_n(x, y)|^2 ds}. \qquad (2)$$

So, a fraction of the mode n, p_n, is calculated as,

$$p_n = \frac{|C_n|^2 \cdot \int_S |\phi_n|^2 ds}{\int_S |A|^2 ds}$$

$$= \frac{|\int_S A(x, y, 0)e^{j\varphi(x,y,0)} \cdot \phi_n^* ds|^2}{\int_S |\phi_n|^2 ds \cdot \int_S |A|^2 ds}. \qquad (3)$$

The eigenfunctions in an over-sized corrugated waveguide with the radius of a are approximately given by [5]

$$\phi_{n,m}^{even} = J_{n-1}\left(X_{n-1,m}\frac{r}{a}\right) \cdot \cos(n-1)\phi$$
$$\text{for } n, m = 1, 2, \cdots$$
$$\phi_{n,m}^{odd} = J_{n-1}\left(X_{n-1,m}\frac{r}{a}\right) \cdot \sin(n-1)\phi \qquad (4)$$
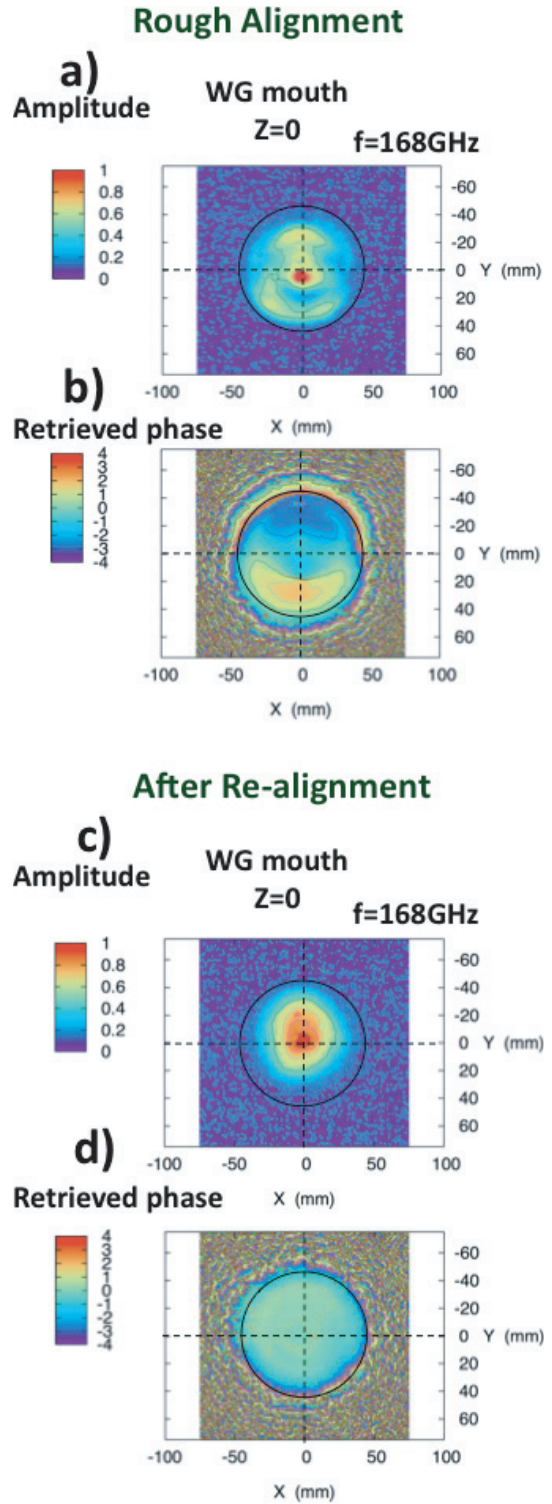$$\text{for } n = 2, 3, \cdots, m = 1, 2, \cdots$$

Fig. 2 Measured amplitudes and retrieved phases at the radiating edge of the corrugated waveguide. The amplitude in a) and phase profile in b) for the rough alignment case. The amplitude in c) and phase profile in d) for the re-alignment case.

Here, $X_{n-1,m}$ are m-th roots of Bessel function $J_{n-1}(X_{n-1,m}) = 0$ and $r = \sqrt{x^2 + y^2}$, $\phi = \tan^{-1}(y/x)$.

This method was applied to the 168 GHz transmission line in the ECH system of LHD. Figure 2 shows measured amplitudes and retrieved phases at the radiating edge of

the circular corrugated waveguide. Figures a) and b) correspond to the amplitude and the phase profiles for the rough alignment case, respectively. Figures c) and d) are the amplitude and phase profiles for the case after re-alignment of the waveguide. In the rough alignment case, the intensity pattern breaks into several peaks and the phase in the lower part is the reverse of that in the upper part on the waveguide cross section. After re-alignment, the intensity profile was improved to be a Gaussian-like one and the phase distribution was almost constant.

These data were used for the mode-content analysis following the above mentioned method. Figure 3 shows the analyzed mode content of both cases in Fig. 2 for the orthogonal even- and odd-modes in the corrugated waveguide. In the rough alignment case, the HE_{11} main propagating mode is only 13%. The major component is the HE_{21} odd mode, which stems from the profile asymmetry with respect to the x-axis as shown in Fig. 2 a) and b). The HE_{12} mode of 18.5% is partly caused by the off-axis components in the amplitude profile. In the re-alignment case, the HE_{11} main propagating mode is recovered to dominate 89% and the other unwanted modes are HE_{21}/1.1%,

HE_{12}/0.9% (even-mode) and HE_{21}/5.4% (odd-mode). The small fraction of the HE_{21} odd mode is attributed to the small offset of the intensity center from the waveguide axis in the y-direction.

3. Field Reconstruction

On the contrary, the electromagnetic field at the arbitrary position, z, in the waveguide can be reconstructed using the expansion coefficients of each eigenmode, $C_n e^{j\varphi_n}$, and the propagation phase factor, $e^{(-j\beta_n z)}$, where β_n is the propagation constant of the mode n in the z-direction.

The amplitude and phase at an arbitrary z position in the corrugated waveguide are generally represented as follows,

$$A(x, y, z)e^{j\varphi(x,y,z)} = A_r(x, y, z) + jA_i(x, y, z) \qquad (5)$$

$$= \sum_{n=1}^{N} C_n e^{j\varphi_n} \phi_n(x, y) \exp(-j\beta_n z), \qquad (6)$$

where

$$\beta_n = \sqrt{k^2 - \left(\frac{X_n}{a}\right)^2}, \qquad (7)$$

$$k = \frac{\omega}{c} = \frac{2\pi}{\lambda}. \qquad (8)$$

ω and λ are the angular frequency and wavelength of a propagating wave, respectively. c is the speed of light. Finally the real and imaginary parts of the wave field, A_r and A_i, are expressed as follows,

$$A_r(x, y, z) = \sum_{n=1}^{N} \Big\{ C_n \cos\varphi_n \cos(\beta_n z) + C_n \sin\varphi_n \sin(\beta_n z) \Big\} \phi_n(x, y). \qquad (9)$$

$$A_i(x, y, z) = \sum_{n=1}^{N} \Big\{ -C_n \cos\varphi_n \sin(\beta_n z) + C_n \sin\varphi_n \cos(\beta_n z) \Big\} \phi_n(x, y). \qquad (10)$$

Figure 4 illustrates the configuration of the field calculations. The z-axis coincides with the waveguide axis. The millimeter-wave from a 168 GHz gyrotron is coupled to the corrugated waveguide at its entrance ($z = -3.2\,\mathrm{m}$) and radiated from the waveguide exit ($z = 0$).

Figure 5 shows the amplitude in a) and phase contour plots in b) of the reconstructed field for the rough

a) Rough Alignment Case

Mode	Even (%)	Odd (%)
HE11	13.289	-
HE12	18.499	-
HE13	0.337	-
HE14	0.584	-
HE15	0.173	-
HE21	0.440	35.709
HE22	0.213	5.897
HE23	0.020	0.451
HE24	0.064	0.986
HE25	0.022	0.218
HE31	13.741	0.723
HE41	0.465	2.542

b) After Re-alignment Case

Mode	Even (%)	Odd (%)
HE11	88.841	-
HE12	0.910	-
HE13	0158	-
HE14	0.118	-
HE15	0.161	-
HE21	1.149	5.357
HE22	0.140	0.684
HE23	0.079	0.131
HE24	0.012	0.086
HE25	0.036	0.177
HE31	0.432	0.048
HE41	0.147	0.021

Fig. 3 Results of the mode-content analysis for even and odd modes in the corrugated waveguide. a) Rough alignment case and b) Re-alignment case.
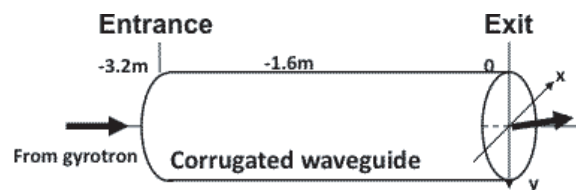

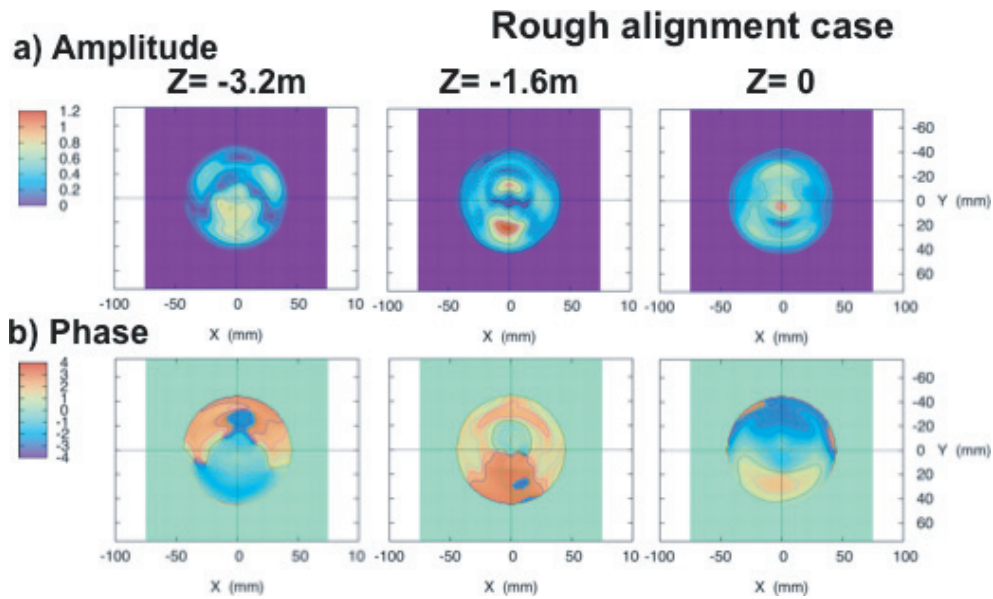Fig. 4 The configuration of the field calculations. The z-axis coincides with the waveguide axis.
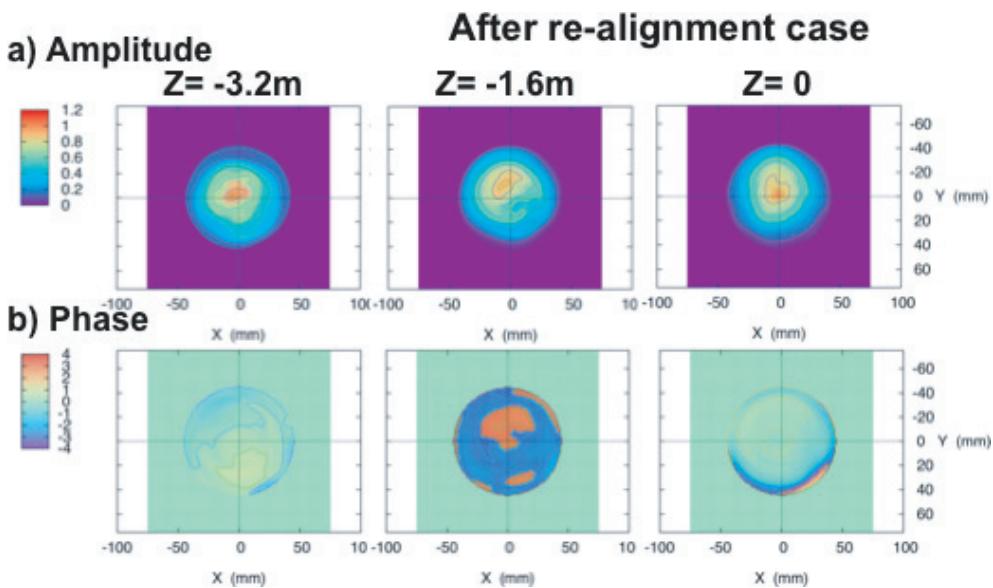
Fig. 5   For the rough alignment case, contour plots of a) the amplitude and b) the phase of the reconstructed electric field at several positions ($z = -3.2$ m, -1.6 m and 0) in the corrugated waveguide.

Fig. 6   For the re-alignment case, contour plots of a) the amplitude and b) the phase of the reconstructed electric field at several positions ($z = -3.2$ m, -1.6 m and 0) in the corrugated waveguide.

alignment case at the entrance, middle and exit positions ($z = -3.2$ m, -1.6 m and 0) as indicated in Fig. 4. The positions of $z = -3.2$ m and $z = 0$ correspond to the entrance and the exit of the corrugated waveguide under test, respectively. Remarkable changes in the amplitude and the phase profiles are observed. A part of the incident millimeter-wave beam seems to hit the waveguide wall at the waveguide entrance.

Figure 6 shows the same contour plots of the amplitude in a) and phase profiles in b) of the reconstructed field for the re-alignment case. The peak position in the amplitude profile moves slightly in the y-direction. This is due

to the existence of the same dominant mode, HE_{21} (odd-mode). The phase profile, however, keeps almost uniform along the waveguide axis.

In general, the n-th moment in the x-direction weighted by the intensity $A(x, y, z)^2$ can be defined as,

$$<x^n> (z) = \int x^n A^2(x, y, z) \mathrm{d}x\mathrm{d}y / \int A^2(x, y, z)\mathrm{d}x\mathrm{d}y.$$

(11)

As a representative of the power density center, the first moment was calculated. The results are shown in Fig. 7. The dashed curves with open symbols represent the
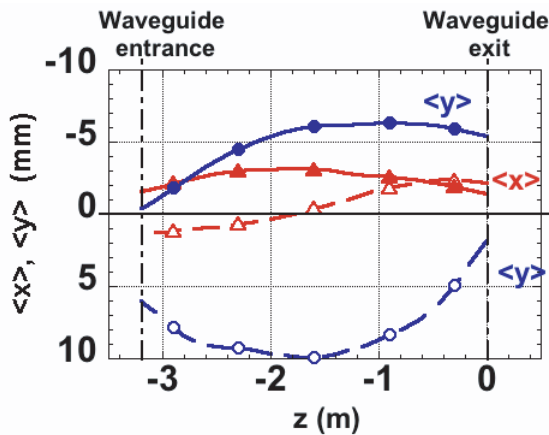
Fig. 7 The first moments of the intensity profiles shown in Figs. 5 and 6. The dashed curves represent the changes in the rough alignment case, and the solid curves represent those in the re-alignment case. The curves with trianglar symbols correspond to the changes in the x-direction, and the curves with circular symbols correspond to those in the y-direction, respectively.

changes of the first moment for the x- and y-directions in the rough alignment case. The solid curves with closed symbols show the changes in the re-alignment case. Because the beat wavelength between the main mode HE_{11} and HE_{21}, which is the most dominant mode among the unwanted modes, is about 9.8 m, the calculated result shows the periodic change of the first moment $< y >$ whose period coincides with about a beat wavelength in both cases. In the x-direction, the non-axisymmetric unwanted even-mode of HE_{21} also affects the value of $< x >$ and shows the same periodic change. Because HE_{12} is an axisymmetric mode, the first moment calculation is not affected by this mode.

In the re-alignment case, the values of $< x >$ and $< y >$ change with the same period, and their periods correspond to the beat wavelength between HE_{11} and HE_{21}. The amplitudes of $< x >$ and $< y >$, however, become smaller than those in the rough alignment case. Although the center of the intensity is located near the waveguide axis at the entrance, the calculated phase profile indicates a little tilting phase profile in the y-direction, which is about 0.3 degree as shown in Fig. 6 b) at $z = -3.2$ m. This seems to cause a generation of the dominant unwanted mode of HE_{21} (odd-mode).

4. Conclusions

The mode content of a high power electromagnetic wave propagating through a corrugated waveguide in an ECH system could be well analyzed using the retrieved phase information, and the wave field in the waveguide was reconstructed on the basis of the complex amplitude of each eigenmode. The advantage of the method is that the data that are used are measured in the same configuration and at the same high power level as in the actual transmission system. The obtained results can be useful to analyze the possible cause of degradation in the transmission efficiency.

The methods of mode-content analysis and field reconstruction were applied to two cases; the roughly aligned waveguide line and the re-aligned waveguide line. The result of the mode-content analysis clearly gives the cause of the misalignment between the incident beam axis and the waveguide axis. Subsequent field reconstruction in the waveguide gives the changes of the field profile and the immeasurable phase information of the wave propagating through the waveguide. In particular, the phase information at the waveguide entrance gives good guidance for waveguide alignment. It became clear that burn-pattern measurements at two positions were insufficient for beam alignment, because the center of the measurable intensity distribution changes with the period of the beat wavelength between the related modes. This suggests that the burn-pattern measurement should be performed, for example, at several positions separated by less than a quarter beat wavelength between the main mode and unwanted modes.

[1] K. Ohkubo, S. Kubo, H. Idei, M. Sato, T. Shimozuma and Y. Takita, Int. J. Infrared Millim. Waves **18**, 23 (1997).
[2] T. Shimozuma, H. Idei, M.A. Shapiro, R.J. Temkin *et al.*, J. Plasma Fusion Res. **81**, 191 (2005).
[3] H. Idei, M.A. Shapiro, R.J. Temkin, T. Shimozuma and S. Kubo, Proc. of the 32nd Int. Conf, on Infrared and Millimeter waves, pp.67-68, MonA3-3 (2007).
[4] M.A. Shapiro, T.S. Chu, D.R. Denison *et al.*, Fusion Eng. Des. **53**, 537 (2001).
[5] N.L. Aleksandrov, A.V. Chirkov, G.G. Denisov and S.V. Kuzikov, Int. J. Infrared Millim. Waves **18**, 1505 (1997).